12.4 Alignment and Manufacturing Tolerances for Segmented Telescopes

Similar to the JWST, the next-generation large-aperture space telescope for optical and UV astronomy has a segmented large deployable primary mirror of 8 to 16 m.[11,12] The astronomer and the optical engineer need to decide how much control authority for the wavefront is on the primary mirror and how much system control authority can be assigned to a second stage of the optical system and thus onto an active or adaptive optics element. Holding and tracking the motion of the primary mirror to a tolerance of 5 nm over a 16-m aperture for diffraction-limited performance in the UV is very difficult and extremely expensive. The telescope designer needs to perform a cost-benefit trade-off study to decide how resources are to be divided between a large segmented primary mirror and the smaller surface on an adaptive optics mirror. Factors that influence this design decision are discussed in this section.

The surface of each mirror segment of a segmented primary mirror must lie on the surface of the desired primary mirror optical prescription. However, each segment is mechanically independent from the others, connected only through a mechanical back plane structure that supports and aligns each individual mirror segment. Adjustments are needed for tip, tilt, piston, off-axis positions, and rotations of each segment. Piston is generally considered along the direction of the ray to the image plane. Some segmented-mirror telescopes use segments with spherical surfaces, which relieve the tolerance of axial position. However, high-quality imaging telescopes, such as the two Keck 10-m telescopes, have an aspheric surface for the primary mirror; therefore, each mirror segment is an aspheric surface with the optical axis off of the surface. These segments with aspheric surfaces require careful alignment.[13–16] The radii of curvaturesof each of the segments must be within a particular tolerance. The value of this tolerance is discussed in the following section.

12.4.1 Curvature manufacturing tolerance

We examine a simple two-segment mirror to describe the tolerances necessary to obtain diffraction-limited performance. To align a segmented aperture, the axes of each segment must be collinear with the axis of the reference conic surface, which passes through the desired focal point, as shown in Fig. 12.6. The reference conic surface is a surface in space on which the surface of each segment is placed to form the primary mirror of the telescope. Recall that all conic surfaces have an axis defined by the line from the vertex of the surface through the focus point.

To calculate the allowable error on the collinearity of the segment axes, we need to imagine that each segment creates its own independent (uncorrelated) image. That is, the angular resolution at the focal plane corresponds to that from only one segment. Next, we bring the axes together and match the radii of curvature of each segment so that an image is formed at the angular resolution of the full aperture across the desired FOV of the system of mirrors that form the segmented primary. The wavefront from each segment is now coherent with that from its neighboring segment, and a high-resolution image is formed.

As the FOV becomes larger, the tolerance to match the radii of curvature becomes tighter to maintain diffraction-limited performance across the field.[17] This can be seen intuitively. The plate scale at the focal plane (for example, in units of seconds of arc per micron) depends on the focal length. The longer the focal length, the larger the image is. Each segment superposes its own image onto that of the others, and we need the image scale and thus the focal lengths to be matched within a certain tolerance.

Figure 12.7 shows a pupil plane of diameter D and two image planes. One image plane, indicated by focal length f_1, is shorter than the second focal plane of focal length f_2. The image plane scale for the two focal lengths is, of course, different; one focal plane is shown larger than the other. The chief ray makes angle α_1 with the axis for the image plane formed by focal length f_1, and the chief ray makes angle α_2 with the axis for the image plane formed at focal length f_2. As an example, we will consider a particular case. Assume that we want $Q = 2$ and that the following system parameters apply:

1. The segmented mirror has an outside diameter D of 10 m.
2. The effective focal length (EFL) of the telescope is 60 m.
3. There are no off-axis aberrations.
4. We use an 8192×8192 pixel focal plane. The FOV radius in units of pixels is given by $\sqrt{2}/2$, which equals 5,792 pixels.
5. The pixels are 4-μm pitch in size, so the FOV radius r, center to edge at the image plane is 23.2 mm.

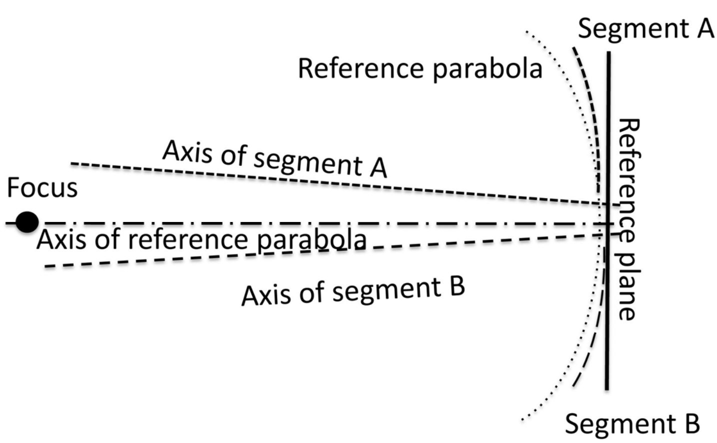

Figure 12.6 Cross-sectional diagram of a two-element segmented telescope. The reference parabola is the dotted curve with its axis passing through the desired focal point. A reference plane that also passes through the focus is shown perpendicular to the axis of the reference parabola. The misalignment of the segments is exaggerated. Segment A is shown with its axis not passing through the focus. The axis of segment B is also shown not passing through the focus.

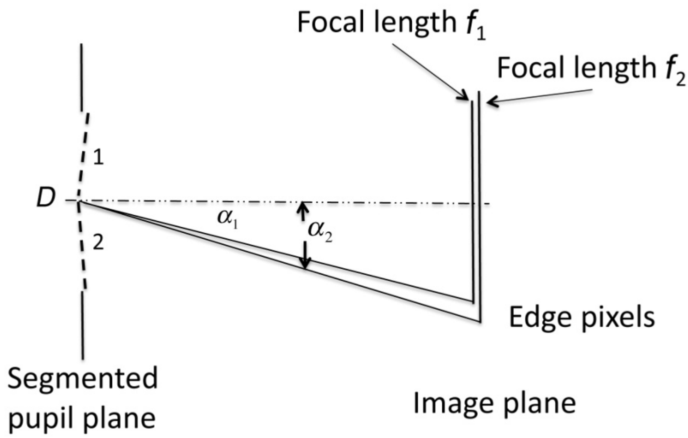

Figure 12.7 A pupil plane of diameter *D* is illuminated from the left. The pupil is segmented with two segments; the focal length of one segment is f_2, and the focal length of the second segment is f_1.

Then, the diameter *d* of the diffraction spot is given by

$$d = \frac{2.44\lambda}{D} \cdot 60 \text{ m} = 7.3 \text{ µm}. \tag{12.12}$$

With 4-µm pixels, $Q \approx 2$ (for reference, see Section 9.11), and if the system is diffraction limited, the pixel sampling of the image is such that diffraction-limited images are recorded.

If r_1 and r_2 are the heights (radius from the axis to the corners) of the image for the system with focal length f_1, and for the system with focal length f_2, respectively, then we can write

$$r_1 = \alpha_1 \cdot f_1 \text{ and } r_2 = \alpha_2 \cdot f_2. \tag{12.13}$$

If we assume that an image quality analysis allows for the 4-µm-square pixel to have an allowable error of 0.2 pixels, then the allowable shear error between the two planes is 0.8 µm at maximum, which is at the corners of the field. Therefore, the image plane scale for the system with focal length f_1 must match the image plane scale for the system with focal length f_2 to within 0.8 µm, and we can write

$$r_1 - r_2 = \Delta r = 0.8 \text{ µm}. \tag{12.14}$$

From Eq. (12.13) we see that $\Delta r = \alpha_2 \cdot f_2 - \alpha_1 \cdot f_1$. It is reasonable to assume that $\alpha_1 \cong \alpha_2 \cong \alpha$; therefore,

$$\Delta r = \alpha \left(f_2 - f_1 \right). \tag{12.15}$$

We see that if

$$\Delta r = \frac{r}{f} \cdot \Delta f, \text{then } \Delta f = \frac{f}{r} \cdot \Delta r. \tag{12.16}$$

Using the values given above, we find that $\Delta f = 2.07$ mm.

If we let f_k be the focal length of the k^{th} segment, and using the term $\langle f \rangle$ to represent the focal length of the ensemble of segments, then

$$\left| \langle f \rangle - f_k \right| < 2.0 \text{ mm}. \tag{12.17}$$

If $\left| \langle f \rangle - f_k \right| > 2.0$ mm, the PSF from one mirror is continuously changing slightly with FOV radius (relative to the other) from the field center to the field edge until, when it reaches the edge, each PSF is separated by > 0.2 pixels. In this case the OTF is not stationary across the image, and the image reconstruction algorithms we considered in Section 9.1 might not be able to reconstruct information at the diffraction limit of the telescope. At a minimum, the PSF of the system—particularly at the extremes of the FOV—is degraded, and the aperture is no longer diffraction limited. In some cases, particularly for a long-exposure recording of an image through turbulence, this may make no difference. However, for a space-based segmented telescope where diffraction-limited imaging may be desired, this is very important.

Let us assume the primary mirror to be *f*/# = 6. For a 10-m-diameter mirror, the focal length is then 60 m, and the radius of curvature is 30 m. Therefore, to build this segmented telescope, we ask that the optician match the radii of curvature of all of the segments to within 2 mm over a distance of 60 m. It is very challenging to make the measurement and to fabricate or figure the surface of each segment to this accuracy while holding the desired mirror figure. In practice, for ground-based telescopes, these segments are either distorted slightly by providing force to warp the surface, or a correction to the wavefront is applied using the principles of two-stage optics and WFSC at a relayed image of the segmented pupil.

Many astronomical applications do not require high angular resolution but rather use the large aperture to collect photons. In this case, the radii of curvature of the segments do not need to be matched as closely as they need to be for diffraction-limited imaging performance.

Today, astronomers are moving toward very large FOVs by tiling the focal plane with array detectors. Note that as the FOV increases, the tolerance on the equality of the radii of curvature of the segments becomes tighter. Comprehensive tolerancing of a segmented telescope prior to manufacture requires setting up each segment as a separate optical system in the computer and then raytracing OPDs to the focal plane for a point on axis and points off axis.

The magnitude of misalignment that is acceptable for image quality is determined by setting up the segmented pupil with phase and amplitude errors on the complex wavefronts and iterating a reference image through the system, including appropriate signal-dependent and signal-independent noise from the detector.

12.4.2 Segmented wavefront corrector

If the second-stage optics contains a wavefront-corrector mirror that is segmented in the pattern of the primary, and if one can adjust the curvatures and the tip-tilt of each segment in this wavefront-corrector mirror, then the tolerances on the large primary mirror can be greatly reduced. However, the rotational degree of freedom and the need to co-align all of the axes of the segments with the design axis of the parent asphere of the primary as a whole must be done on the primary. Approaches to segmenting the wavefront-corrector mirror to match the primary have been suggested by several optical scientists[18] and astronomers.[19,20]

12.5 Image Quality with a Segmented Telescope

12.5.1 Image quality

Image quality from large segmented astronomical telescopes has been studied for both ground and space applications.[21–23] Studies on segmented-mirror ground astronomical telescopes have been performed assuming that the active control of tip, tilt, piston, and shape of each segment is independent of its neighbor. Analyses have been done considering the compounding effects of atmospheric turbulence.[24,25] Several groups are building segmented-telescope simulators for calculating PSFs and related metrics such as Strehl ratio, encircled energy, and MTF for both ground- and space-based segmented telescopes.

The diffraction effects for large numbers of segments were analyzed for Strehl ratio. A speckle pattern and a speckle halo were derived and observed.[22] The relationship between the number of segments and the characteristics of the multiconjugate adaptive optics system shows that the Strehl ratio is limited to 0.5–0.7 for operation in the center of the H band at 1650 nm.[26] In Section 12.5.2 we will discuss the correction of errors in segmented telescopes based on the material developed by Meinel and Meinel.[6]

12.5.2 Correcting errors in a segmented telescope with two-stage optics

The individual segments of a large lightweight segmented primary mirror have both a piston error and a tilt error. In this section we assume the segmented surface to be a rigid body, and we consider the effects on telescope system performance caused by piston errors, field-angle errors, tilt errors, and diffraction spillover. The image of the primary on the corrector is demagnified, often somewhere between a factor of 10 and 100. Field of view as a function of this demagnification is discussed in this section.